

PROCEEDINGS OF SPIE

SPIDigitalLibrary.org/conference-proceedings-of-spie

Compact entanglement sources for portable quantum information platforms

Tiphaine Kouadou, Colin Lualdi, Spencer Johnson, Kristina Meier, Josh Aller, et al.

Tiphaine Kouadou, Colin P. Lualdi, Spencer Johnson, Kristina Meier, Josh Aller, Brad Slezak, Tony Roberts, Phil Battle, Paul G. Kwiat, "Compact entanglement sources for portable quantum information platforms," Proc. SPIE 12015, Quantum Computing, Communication, and Simulation II, 120150D (1 March 2022); doi: 10.1117/12.2609989

SPIE.

Event: SPIE OPTO, 2022, San Francisco, California, United States

Compact entanglement sources for portable quantum information platforms

Tiphaine Kouadou^{*a}, Colin P. Luaidi^a, Spencer Johnson^a, Kristina Meier^b, Josh Aller^c, Brad Slezak^c, Tony Roberts^c, Phil Battle^c and Paul G. Kwiat^a

^aDepartment of Physics, Illinois Quantum Information Science and Technology Center (IQUIST),
University of Illinois Urbana-Champaign, Urbana, IL 61801;

^bLos Alamos National Laboratory, Los Alamos, NM 87545; ^cAdvR Inc., Bozeman, MT 59715

ABSTRACT

We discuss two novel entanglement sources utilizing spontaneous parametric downconversion in periodically poled waveguides. Using quasi-phase matched KTP crystals, we have demonstrated a post-selection-based polarization-entangled degenerate source at 810 nm, as well as a post-selection-free non-degenerate collinear source producing entangled photons at 810 nm and 1550 nm. The sources exhibit high brightness and state quality – with the non-degenerate source achieving fidelities and purities up to 99% – with clear paths for further improvement. Furthermore, they are compact, stable, and need little alignment when set, critical for practical quantum communication and network applications. Lastly, their small size, weight, and power (SWaP) makes them an attractive option for mobile platforms, e.g., with drones or satellites.

Keywords: quantum information, entanglement, space-based quantum cryptography, nonlinear optics, compact sources

1. INTRODUCTION

Quantum communication [1] is a field of great scientific and technological interest, with applications in secure quantum communications [2-7], quantum sensing [8], and distributed [9,10] and remote quantum computing [11]. The grand challenge is to establish a quantum network [5] that could allow quantum communications on a global scale. Existing terrestrial schemes, in free-space or in fiber, are based on the transmission and detection of single photons or pairs of entangled photons, but attenuation and detection noise limit quantum communication links to hundreds of kilometers [12]. Satellite-based systems would help overcome these limitations [4,7], by allowing the transmission of single photons and pairs of entangled photons in vacuum, therefore enabling quantum communication over larger distances than what is possible with ground-based schemes. Indeed, implementing such sources on drones would allow for reconfigurable quantum networks close to the ground. Spontaneous parametric downconversion (SPDC) in nonlinear crystals has become a reliable option to create pairs of entangled photons. In addition, using waveguides allows sources of high brightness, due to the high intensity caused by light confinement. Multiple groups have presented waveguide-based sources of degenerate and near-degenerate polarization entanglement [13-15]. However, highly nondegenerate polarization entanglement using SPDC has been proposed [16], but not experimentally demonstrated from a waveguide source. We developed such a source in collaboration with AdvR Inc., with the goal to realize a bright, compact, and stable source suitable for advanced quantum communication protocols. We characterized two types of waveguide sources of entangled photons, a degenerate one, producing orthogonally polarized photons at 810 nm, and a highly non-degenerate source producing polarization-entangled states of photons at 810 nm and 1550 nm. The degenerate source might be optimal for applications where both photons must be transmitted through free space, while the non-degenerate one would enable the telecom wavelength at 1550 nm to propagate through a low-loss optical fiber, thus connecting a wireless free-space quantum network to a fiber-based one.

*tiphaine@illinois.edu

2. POST-SELECTED SOURCE OF ENTANGLEMENT IN A WAVEGUIDE

2.1 Polarization-Entanglement Generation from Degenerate SPDC

Compact SPDC sources are promising for the development of portable quantum communication nodes. An SPDC source with a downconversion wavelength at 808 nm can be readily pumped using small laser diodes. Moreover, 808-nm photons propagate through the atmosphere with low transmission loss and can be detected using Silicon avalanche photodiodes (Si-APDs), which are small, lightweight and operate with only modest cooling. Using a waveguide-based source ensures low size, weight, and power (SWaP), making it suitable for small platforms, e.g., drones or small satellites. Our collaborators at AdvR, Inc. developed such an integrated periodically poled KTP source, using type-II phased-matched SPDC to produce degenerate and orthogonally polarized photon pairs. An external 50/50 beam splitter and post-selection via coincidence measurements allow one to generate a polarization-entangled state. Specifically, if two identical photons in the polarization state $|H_{808}V_{808}\rangle$ are incident on a 50/50 beam splitter, considering only the cases (50%) where one photon is transmitted and the other is reflected, the following post-selected polarization-entangled state is generated:

$$|\psi^+\rangle = \frac{1}{\sqrt{2}} (|H\rangle_r |V\rangle_t + |V\rangle_t |H\rangle_r), \quad (1)$$

where r and t denote the reflected and transmitted ports of the balanced beam splitter. Note that this description implicitly assumes the initial photons cannot be in any way distinguished, e.g., by spatial mode, frequency, or arrival time at the beam splitter. Also, note the state (1) is actually immune to any polarization-dependent loss or phase that occurs before the beam splitter, as these simply appear as global factors multiplying the entire state; it is also robust against polarization-independent imbalance of the beam splitter, which would reduce the rate of coincidences, but not the entanglement quality.

2.2 Experimental Setup

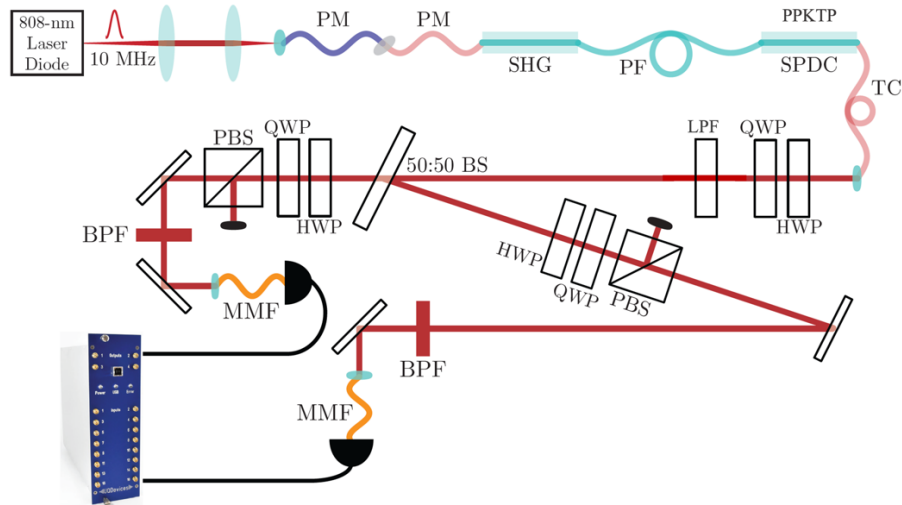


Figure 1. Experimental setup for the degenerate beam splitter polarization-entanglement source. PM: polarization-maintaining fiber; TC: temporal compensation fiber; HWP: half waveplate; QWP: quarter waveplate; LPF: longpass filter; PBS: Polarizing beam splitter; BPF: bandpass filter; MMF: multimode fiber.

Our SPDC pump originates in a volume-holographic-grating (VHG)-stabilized diode laser that is controlled by a pulse driver so as to generate 5 mW of pulsed light centered at 808 nm, with a repetition rate of 10 MHz and pulse duration of 2.5 ns. The output beam is collimated and coupled into a polarization-maintaining (PM) fiber (Fig. 1), which is connected to a second PM fiber pigtailed to a magnesium-doped lithium niobate ridge waveguide in which second harmonic generation (SHG) occurs. This process produces the 404-nm pump light for the subsequent parametric downconversion

process¹; the coupling efficiencies of 808-nm and 404-nm light through the SHG waveguide are 54% and 33%, respectively. For this specific source, the peak SHG conversion efficiency is 46%/W, resulting in an estimated output of 12.5 μ W, close to our measured 10 μ W of 404-nm pump light at the exit of the SHG module.

The output of the SHG waveguide is pigtailed into an additional PM fiber. Because this fiber is single-mode for 404-nm light, most of the 808-nm light is forced into the fiber cladding, where it is easily removed via fiber mode-stripping, by tightly wrapping the fiber around a 1-cm diameter post. After the filtering, the output fiber guides the 404-nm photons into a periodically poled KTP (PPKTP) waveguide where nominally degenerate SPDC occurs. The 404-nm coupling efficiency through the SPDC module is 50% and the 808-nm out-coupling efficiency is 58%. Using type-II phase-matching, the downconverted photons are produced with orthogonal polarizations, i.e., in the state $|H_{808}V_{808}\rangle$, where we explicitly omit the temporal part of the wavefunction, which would show the H-polarized photon exiting the waveguide source ahead of the V-polarized photon, due to birefringent group velocity walk-off created within the 6.5-mm long waveguide. The two photons are guided into a PM fiber that is pigtailed to the PPKTP output facet and cut to a length that fully compensates for this temporal walkoff, thus alleviating the need for additional compensation after the SPDC module. The exiting downconverted photons (and residual pump photons at 404 nm) are collimated with an aspheric lens (11-mm focal length and coated for 800-nm light) and emitted into free-space. We use a HWP and QWP to compensate for any additional unitary polarization rotation caused by the output fiber; the 404-nm pump light is then filtered out with a longpass filter. Finally, a 50/50 beam splitter separates the 808-nm photons into two paths, one transmitted and one reflected. The light from each port is coupled into a multimode fiber and detected with a silicon APD with 60% efficiency; the counts measured by the APDs are processed using a UQDevices Logic16 timetagger and a computer.

2.3 Results

We perform a two-qubit state tomography to characterize the generated states, using a half waveplate, quarter waveplate and polarizing beam splitter on each beam path to analyze the quantum state in the H/V, D/A and R/L bases. This source generates states of $83.9 \pm 0.8\%$ purity, $82.5 \pm 0.9\%$ concurrence and $89.4 \pm 0.8\%$ fidelity with the ideal state (1). These results were obtained after optimizing the temperature of the SPDC waveguide to 31.8°C. At other temperatures, the H and V photons are no longer degenerate, so the entanglement quality degrades. We believe that using narrowband spectral filtering of the state can help further improve the quality of the generated entangled state, if the coincidence counts are not reduced too much by the filtering. In particular, because any difference in the spectra of the originally produced H and V photons will effectively remove the coherence between the two terms in Equation (1), a narrow spectral filter should improve the photon's spectral overlap and thus the entanglement of the post-selected state.

3. DIRECT SOURCE OF NON-DEGENERATE ENTANGLEMENT IN A WAVEGUIDE

3.1 Non-Degenerate SPDC in dually poled waveguides

The non-degenerate polarization-entangled sources, also created by AdvR Inc., were designed for type-II phase-matched SPDC, producing photons at 810 nm and 1550 nm from a bright continuous-wave (CW) pump laser at 532 nm. To create entangled states from a single periodically poled waveguide, we combine two independent SPDC processes inside the same crystal. One process has a poling period of $\Lambda_1 = 27 \mu\text{m}$ and generates the state $|H_{810}V_{1550}\rangle$; the second process has a poling period of $\Lambda_2 = 58 \mu\text{m}$ and generates the state $|V_{810}H_{1550}\rangle$. In principle, one could produce the same states with two separate crystals, but using a single crystal avoids coupling losses between the two crystals. Because of this geometry, when the photon pairs from each source exit the device, we have no information about which source each photon came from, generating the following entangled state:

$$|\psi\rangle = \frac{1}{\sqrt{2}} (|H_{810}V_{1550}\rangle + |V_{810}H_{1550}\rangle). \quad (2)$$

As with (1), (2) omits the effect of birefringent walkoff from the different propagation speeds of the different polarizations and wavelengths (including the pump) inside the waveguide; this must be compensated by including extra birefringent

¹ Alternatively, one could pump the waveguide directly, e.g., using a 404-nm frequency-stable diode laser.

elements in both photons' paths. Note that we can either juxtapose the two processes inside the nonlinear waveguide ("adjacent" source) or interleave them ("interleaved" source); both approaches in principle create the same entangled state, but in practice the required optimal temporal compensation is different and as we shall see, the "interleaved" source displayed poorer performance.

3.2 Experimental Setup

Our non-degenerate waveguide source (Fig. 2) is pumped with a CW 532-nm beam, frequency doubled from a Nd:YAG laser at 1064 nm. The diverging 532-nm beam is collimated to an approximate diameter of 1 mm and travels through a half waveplate, quarter waveplate and polarization beam splitter (PBS) to set the polarization state to horizontal (H). Then the beam is coupled into a polarization-maintaining (PM) single-mode fiber glued to the input of the waveguide; a half waveplate is used to finely adjust the pump polarization to match the stable polarization axis of the PM fiber. Fiber-pigtailling the input waveguide allows one to stabilize the input mode of the pump, ideally only coupling to the fundamental mode of the waveguide and thereby improving the net stability of the source², a 16-mm long and 4- μ m-deep channel PPKTP waveguide. Because the waveguide is created at the surface of the crystal, the refractive index difference with the air is much higher at the top of the waveguide than between the rest of the waveguide and the surrounding bulk KTP. For this reason, the actual, somewhat rectangular, fundamental mode of the waveguide does not have the circular symmetry of a gaussian mode, leading to coupling losses between the mode of the waveguide and the mode of the pump beam.

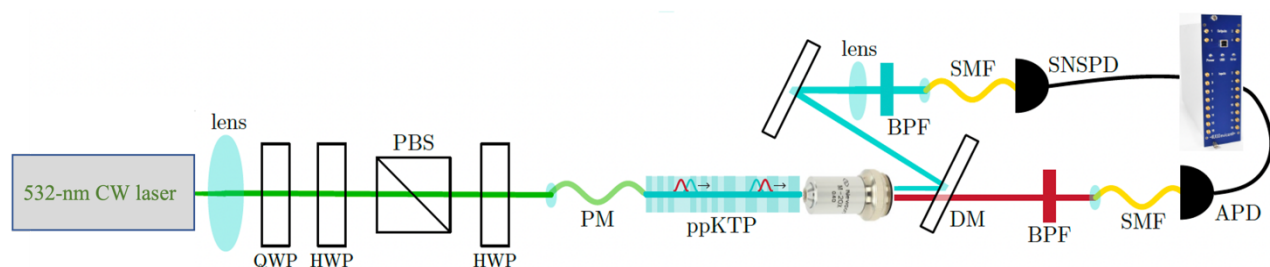


Figure 2. Experimental setup of the non-degenerate source of entangled photons. SMF: single-mode fiber; BPF: bandpass filter; PM: polarization-maintaining fiber; DM: dichroic mirror; HWP: half waveplate; QWP: quarter waveplate; PBS: Polarizing beam splitter; SNSPD: Superconducting Nanowire Single Photon Detector; APD: Avalanche Photodiode.

At the waveguide output, we use a 20x microscope objective with a focal length of 9.0 mm and numerical aperture (NA) of 0.4 to collimate the beam (due to the wavelength dependence of the objective focal length, we use a secondary lens to fix the collimation of the 1550-nm output beam). After the microscope objective, longpass filters remove the 532-nm pump, and a dichroic mirror separates the downconversion beams by wavelength, letting the 810-nm beam and any residual 532-nm pump through and reflecting the 1550-nm light. After the dichroic mirror, bandpass filters (two in the 810-nm path and one in the 1550-nm path) allow for additional filtering; this is also where additional calcite crystals in the two arms (not shown in Fig. 2) compensate the relative temporal walkoff of the SPDC photons. The downconversion photons are coupled into single-mode fibers and detected in coincidence on separate detectors. For the "adjacent" source, the 810-nm photons were detected with a Si-APD from Excelitas (~60% detection efficiency), and the 1550-nm photons detected using a cryogenically cooled Superconducting Nanowire Single Photon Detector (SNSPD, ~90% detection efficiency); for the "interleaved" source both 810-nm and 1550-nm photons were detected with SNSPDs. As with the degenerate source setup, the detector output signals are processed via the QDevices timetagger.

3.3 Spectral Filtering and Waveguide-Temperature Tuning

We can use coincidence measurements to compare the spectra of the $|H_{810}V_{1550}\rangle$ and $|V_{810}H_{1550}\rangle$ processes; we couple the single-mode fiber collecting the 1550-nm photons to a tunable filter with 0.05-nm tuning resolution and measure the

² The size of the waveguide is fixed by the size of the fundamental mode of the longest wavelength traveling through it, in our case, 1550 nm. Consequently, the waveguide is actually multimode for the 532-nm pump beam. The multimode nature of the pump inside the waveguide can cause complexity in the higher-order downconversion spectrum.

coincidence counts as a function of the central filter wavelength for both processes. The two processes can be optimized for different settings of the tunable filter, and we can seek to overlap them by tuning the temperature of the waveguide (Fig. 3) (using a Vescent temperature controller with mK precision). Indeed, the phase-matching is optimal for a given temperature, which depends on the pump and downconversion wavelengths, the nonlinear material (here KTP), and the geometry of the waveguide.

The states generated from the adjacent and interleaved source configurations were characterized the same way as the degenerate source, via state tomography, performed for several temperatures of the SPDC waveguide. For the adjacent SPDC source, we found the best results at 37°C: $99.0 \pm 0.5\%$ state purity, $98.6 \pm 0.5\%$ state fidelity and $98.3 \pm 0.4\%$ concurrence; for the interleaved source, we ran tomographies for several crystal temperatures and at several settings of the tuning filter. The best preliminary results are $89.8 \pm 0.6\%$ state purity, 87.3% state fidelity and $86.6 \pm 0.7\%$ concurrence, at 21°C. From these experiments, the adjacent source appears to give the best results.

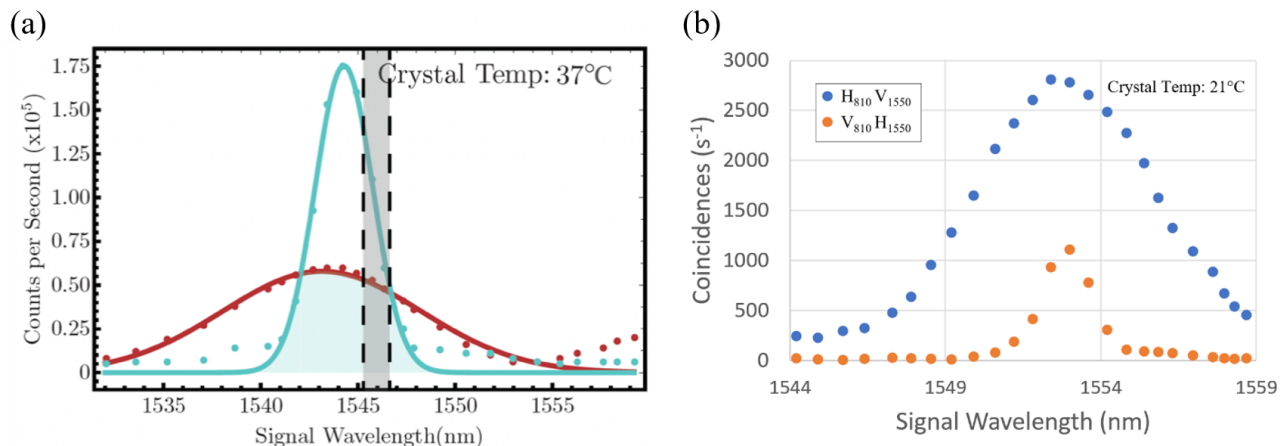


Figure 3. Comparison of the spectra of the processes generated by the two waveguide SPDC sources. (a) Adjacent source at 37°C; Red: $V_{810}H_{1550}$; Blue: $H_{810}V_{1550}$; (b) Interleaved SPDC source at 21°C.

4. DISCUSSION

Beyond the waveguide approaches we discussed in this manuscript, multiple geometries can be considered to create SPDC-based sources of polarization-entangled photon pairs using, e.g., Sagnac interferometers [17] and beam displacers [18]. These three geometries each have their own advantages – the waveguide sources are brighter (generate more pairs per second per milliwatt of pump power) than bulk sources and their small dimensions are ideal for applications with stringent weight requirements; beam-displacer-based sources alleviate the need for compensation of the group velocity walk-off, and Sagnac-interferometer-based sources are well established and have given good results on complicated experiments such as the distribution of entanglement from space to Earth, but require in-situ alignment [7]. Our goal here was to characterize a waveguide as a viable and potentially superior approach for some applications, particularly these requiring a scalable low-SWaP solution, e.g., to perform quantum communication protocols between drones. Here, small plug-and-play devices capable of producing photon pairs at high rates would be ideal to tolerate high transmission losses. Moreover, such devices must require little post-fabrication adjustment, remaining stably aligned with time. This would also make them a critical resource for future satellite-based quantum communication, as they would need to be able to survive a rocket launch without need for remote re-alignment.

For example, an entanglement source could be located on a satellite in orbit; an 810-nm photon could remain on the satellite detected by Si-APDs, while the 1550-nm sister photon could be collected at a ground station on Earth and measured using more efficient SNSPDs. The advantage of using telecom wavelength for collection on Earth is that the required infrastructure for sending this wavelength between Earth stations and satellites already exists. In other communication applications on the ground, the longer wavelength can be transmitted with minimum loss through optical fibers, while the shorter wavelength can be more easily coupled to some quantum memory platforms.

In the measurements presented here, we cared only about the quality of the (polarization) entanglement. However, for many future applications – teleportation, entanglement swapping, quantum repeaters – one must also require the photons not to be entangled in any other degree of freedom (e.g., spectral). Such ancillary entanglement would prevent the 2-photon interference required for these other operations. Fortunately, it should be possible to achieve such spectrally factorizable states by careful pump and SPDC engineering; this will be the subject of future investigations.

ACKNOWLEDGEMENTS

This research was supported by NASA Grant No. NNX16AM26G, NASA SBIR Contract 80NSSC18C0030, and U.S. Air Force STTR Contract FA864921P0774.

REFERENCES

- [1] Gisin N., Thew R., “Quantum Communication”, *Nat. Phot.* 1, 165–171 (2007)
- [2] Bennett C. H. and Brassard G., in *Proceedings of the IEEE International Conference on Computers, Systems, and Signal Processing*, Bangalore, India, IEEE, New York, p. 175 (1984)
- [3] Autebert. C et al., “Multi-user quantum key distribution with entangled photons from an AlGaAs chip”, *Quantum Sci. Technol.* 1, 01LT02 (2016)
- [4] Yin J. et al., “Satellite-to-Ground Entanglement-Based Quantum Key Distribution”, *Phys. Rev. Lett.* 119, 200501 (2017)
- [5] Wehner S., Elkouss D., and Hanson R., “Quantum Internet: A vision for the road ahead”, *Science* 362, 6412 (2018)
- [6] Shi Y., Thar S. M., Poh H. S., Grieve J. A., Kurtsiefer C., and Ling A., “Stable polarization entanglement-based quantum key distribution over a deployed metropolitan fiber”, *Appl. Phys. Lett.* 117, 124002 (2020)
- [7] Yin J. et al., “Entanglement-based secure quantum cryptography over 1,120 kilometres”, *Nature* 582, 501-505 (2020)
- [8] Zhang Z., and Zhuang Q., “Distributed Quantum Sensing”, *Quantum Sci. Technol.* 6 043001 (2021)
- [9] Van Meter R., and Devitt S. J., “The Path to Scalable Distributed Quantum Computing” in *Computer* 49, 31-42 (2016)
- [10] Gyongyosi L., and Imre S. “Scalable distributed gate-model quantum computers”, *Sci. Rep.* 11, 5172 (2021)
- [11] Fitzsimons J. F., “Private quantum computation: an introduction to blind quantum computing and related protocols”, *npj Quant. Info.* 3, 23 (2017)
- [12] Korzh B., Lim C., Houlmann R. et al., “Provably secure and practical quantum key distribution over 307 km of optical fibre”, *Nature Photon* 9, 163–168 (2015)
- [13] Suhara T., Nakaya G., Kawashima J., and Fujimura M., “Quasi-phase-matched waveguide devices for generation of postselection-free polarization-entangled twin photons”, *IEEE Phot. Tech. Lett.* 21, 1096 (2009)
- [14] Kuo P. S., Verma V. B., and Nam S. W., “Demonstration of a polarization-entangled photon-pair source based on phase-modulated PPLN” *OSA Continuum* 3, 295-304 (2020)
- [15] Kang D., Zareian N., and Helmy A. S., in *Advances in Photonics of Quantum Computing, Memory, and Communication XI*, SPIE 10547, 67-73 (2018)
- [16] K. Thyagarajan et al., “Generation of polarization-entangled photons using type-II doubly periodically poled lithium niobate waveguides”, *Phys. Rev. A* 80, 052321 (2009)
- [17] Kim T., Fiorentino M., and Wong F. N. C., “Phase-stable source of polarization-entangled photons using a polarization Sagnac interferometer”, *Phys. Rev. A* 73, 012316 (2006)
- [18] Hentschel M., Hübel H., Poppe A., and Zeilinger A., “Three-color Sagnac source of polarization entangled photon pairs”, *Opt. Express* 17, 23153 (2009)